Molecular Pharmacology Fast Forward. Published on January 3, 2017 as DOI: 10.1124/mol.116.106161
This article has not been copyedited and formatted. The final version may differ from this version.

Title page

Crosstalk between alternatively spliced UGT1A isoforms and colon cancer cell metabolism

Yannick Audet-Delage, Michèle Rouleau, Mélanie Rouleau, Joannie Roberge, Stéphanie Miard, Frédéric Picard, Bernard Têtu and Chantal Guillemette

Pharmacogenomics Laboratory, Centre Hospitalier Universitaire de Québec (CHU de Québec) Research Center and Faculty of Pharmacy, Laval University, Québec, Canada (YAD, MiR, MeR, JR, CG).

Centre de recherche de l'Institut universitaire de cardiologie et de pneumologie de Québec (CRIUCPQ), Laval University, Québec, QC, Canada (SM, FP)

Centre Hospitalier Universitaire de Québec (CHU de Québec) Research Center and Faculty of Medicine, Laval University, Québec, Canada (BT)

Molecular Pharmacology Fast Forward. Published on January 3, 2017 as DOI: 10.1124/mol.116.106161
This article has not been copyedited and formatted. The final version may differ from this version.

Running Title: Alternative UGT1A and cancer cell metabolism

CORRESPONDING AUTHOR:

Chantal Guillemette, Ph.D. Canada Research Chair in Pharmacogenomics

CHU de Québec Research Center, R4720, 2705 Boul. Laurier, Québec, Canada, G1V 4G2. Phone: (418) 654-2296

Email: chantal.guillemette@crchudequebec.ulaval.ca

Number of text pages: 18

Number of tables: 0

Number of figures: 6

Number of references: 61

Word count:

Abstract: 243

Introduction: 1027

Discussion: 1404

Molecular Pharmacology Fast Forward. Published on January 3, 2017 as DOI: 10.1124/mol.116.106161
This article has not been copyedited and formatted. The final version may differ from this version.

List of abbreviations:

CAT, catalase; co-IP, co-immunoprecipitation; CTR, control; ECAR, extracellular acidification rate; FBS, fetal bovine serum; FCCP, trifluoromethoxy carbonylcyanide phenylhydrazone; i1, isoform 1; i2, isoform 2; KD, knockdown; OCR, oxygen consumption rate; OXPHOS, mitochondrial oxidative phosphorylation; PBS, phosphate buffered saline; PKM, pyruvate kinase; PRDX1, peroxiredoxin 1; RQ, relative quantities; UDPGlcA: UDP-glucuronic acid; UGT, UDP-glucuronosyltransferase; TCA, tricarboxylic acid cycle

Molecular Pharmacology Fast Forward. Published on January 3, 2017 as DOI: 10.1124/mol.116.106161
This article has not been copyedited and formatted. The final version may differ from this version.

Abstract

Alternative splicing at the human glucuronosyltransferase 1 gene locus (*UGT1*) produces alternate isoforms UGT1A_i2s that control glucuronidation activity through protein-protein interactions. Here, we hypothesized that UGT1A_i2s function into a complex protein network connecting other metabolic pathways with influence on cancer cell metabolism. This is based on a pathway enrichment analysis of proteomic data that identified several high-confidence candidate interaction proteins of UGT1A_i2 proteins in human tissues, namely the rate-limiting enzyme of glycolysis pyruvate kinase (PKM), which plays a critical role in cancer cell metabolism and tumor growth. The partnership of UGT1A_i2 and PKM2 was confirmed by co-immunoprecipitation in the HT115 colon cancer cells and was supported by a partial co-localization of these two proteins. In support of a functional role for this partnership, depletion of UGT1A_i2 proteins in HT115 cells enforced the Warburg effect with higher glycolytic rate at the expense of mitochondrial respiration, and led to lactate accumulation. Untargeted metabolomics further revealed a significantly altered cellular content of 58 metabolites including many intermediates derived from the glycolysis and TCA cycle pathways. These metabolic changes were associated with a greater migration potential. The potential relevance of our observations is supported by the down-regulation of UGT1A_i2s mRNA in colon tumors compared to normal tissues. Alternate UGT1A variants may thus be part of the expanding compendium of metabolic pathways involved in cancer biology directly contributing to the oncogenic phenotype of colon cancer cells. Findings uncover new aspects of UGT functions diverging from their transferase activity.

Molecular Pharmacology Fast Forward. Published on January 3, 2017 as DOI: 10.1124/mol.116.106161
This article has not been copyedited and formatted. The final version may differ from this version.

Introduction

The uridine diphospho-glucuronosyltransferases (UGTs) are critical enzymes involved in drug and carcinogen metabolism as well as in the homeostasis of a wide range of endogenous molecules such as bilirubin, steroids and lipids (Rouleau et al., 2014; Rowland et al., 2013). UGT enzymes catalyze the transfer of the sugar moiety of uridine diphospho-glucuronic acid (UDPGlcA) to numerous lipophilic substrates, and this reaction leads to inactivation and favors elimination of metabolites through bile and urine. Together with other metabolizing enzymes and transporters, UGTs are increasingly recognized as key determinants of the interindividual variability in pharmacokinetic and pharmacodynamic outcomes of clinically important drugs (Stingl et al., 2014). Findings also reveal that metabolic alterations in the glucuronidation pathway may determine the degree of exposure of an individual to toxic or carcinogenic substances over a long period determining individual susceptibility to diseases such as cancer, as well as its progression (Rouleau et al., 2014).

Alternative splicing is a powerful mean of controlling gene expression but also creates novel proteins with distinct structural and functional features (Biamonti et al., 2014). Extensive analysis of human *UGT* genomic sequences by our group uncovered a new class of UGT alternate isoforms derived from the *UGT1* locus. Novel transcripts are created by the inclusion of an alternative terminal exon (exon 5b) that leads to the production of nine shorter UGT1A proteins called isoforms 2 (or i2s) (Girard et al., 2007; Levesque et al., 2007). Expression analyses revealed that UGT1A enzymes (referred to as isoforms 1 or i1s) and alternate UGT1A_i2s are co-produced in the same tissue structures of the liver, kidney, stomach, intestine and colon (Bellemare et al., 2011). The

Molecular Pharmacology Fast Forward. Published on January 3, 2017 as DOI: 10.1124/mol.116.106161
This article has not been copyedited and formatted. The final version may differ from this version.

presence of exon 5b in the mRNA sequence causes a premature end of translation, and produces nine alternate UGT1A_i2s with different N-terminal regions (encoded by different exons 1) and lacking the transmembrane domain but comprising ten novel C-terminal amino acids (R_{435}KKQQSGRQM_{444}). As a consequence, these alternate proteins lack transferase function with UDPGlcA but gain new biologic activity by negatively modulating cellular glucuronidation through direct protein-protein interaction with UGT1A enzymes. This represents a new mode of regulation of the UGT metabolic pathway (Bellemare et al., 2010a; Rouleau et al., 2014).

Alternative splicing was shown to produce isoforms with vastly different interaction profiles (Yang et al., 2016). Literature supports oligomerization of UGT enzymes and with other proteins such as cytochrome P450 (Miyauchi et al., 2015; Rouleau et al., 2014). It raises the possibility of other cellular functions for alternate UGT1A proteins and perhaps, in disease processes like cancer. Indeed, the human protein interactome is of pivotal importance in the regulation of biological systems and was shown to contribute to different pathologies, particularly cancer (Mitsopoulos et al., 2015; Yang et al., 2016). These interactions are considered as promising therapeutic targets with selected protein–protein interaction inhibitors that have reached clinical development (Scott et al., 2016). Previous untargeted proteomic experiments with human liver and kidney normal tissues revealed a partnership between UGT1A_i2s and enzymes of the scavenging pathway such as catalase (CAT) and peroxiredoxin (PRDX). By these interactions, UGT1A_i2 proteins likely interfere with oligomeric complex formation necessary for scavenging activity of CAT and PRDX (Rouleau et al., 2014). Other proteins were identified as partners of UGT1A_i2s in human tissues, using an antibody that recognized

Molecular Pharmacology Fast Forward. Published on January 3, 2017 as DOI: 10.1124/mol.116.106161
This article has not been copyedited and formatted. The final version may differ from this version.

all nine alternative UGT1A_i2 proteins but not the nine UGT1A enzymes, including the multifunctional protein pyruvate kinase (PKM). PKM plays a critical role in cancer cell metabolism and tumor growth (Gupta and Bamezai, 2010). However, the potential influence of this crosstalk remains unknown. Besides, it also remains undefined which of the nine UGT1A_i2 proteins interact with these other proteins. We thus postulated that UGT1A_i2s might interact with PKM and influence its activity with potential consequences on cancer cell phenotypes given the role the PKM enzyme in the metabolic remodelling of cancer cells.

Cancer cells present a distinct metabolic phenotype also known as the Warburg effect (Li and Zhang, 2016; Warburg et al., 1927). In this context, the splice variant of pyruvate kinase M2 (PKM2) has received great attention as the major PKM isoform expressed by dividing cancer cells (Anastasiou et al., 2012; Israelsen and Vander Heiden, 2015; Taniguchi et al., 2015). In contrast, PKM1 is more abundant in healthy quiescent cells (Bluemlein et al., 2011; Zhan et al., 2015). PKM2 is a rate limiting glycolytic enzyme and a key metabolic regulator, whereas a clear picture of its function in cancer is still unresolved (Israelsen and Vander Heiden, 2015). PKM2 favors aerobic glycolysis, in which glucose is preferentially catabolized to lactate, rather than fully metabolized to carbon dioxide via mitochondrial oxidative phosphorylation (OXPHOS) (Christofk et al., 2008a). This process provides cancer cells with energy and precursors for the synthesis of nucleic acids, amino acids, and lipids to support cell division. Recent data indicate that overexpression of PKM2 in colon tumors connote poor outcome, as it is associated with advanced tumor stage and lymph node metastasis, and is essential for the aerobic

Molecular Pharmacology Fast Forward. Published on January 3, 2017 as DOI: 10.1124/mol.116.106161
This article has not been copyedited and formatted. The final version may differ from this version.

glycolysis of colon cancer cells *in vitro* (Cui and Shi, 2015; Yang et al., 2014; Yang et al., 2015; Zhou et al., 2012).

In this work, we sought to expose potential metabolic and phenotypic changes associated with UGT1A_i2 proteins in a colon cancer cell model HT115, in which PKM2 is expressed in addition to several different UGT1A proteins, including UGT1A enzymes and alternative i2 isoforms. We initially confirmed the direct interaction of UGT1A_i2s with pyruvate kinase by co-immunoprecipitation (co-IP) in HT115 cell lysates. Compared to normal colon tissues, downregulation of UGT1A_i2s mRNA expression was established in colon tumors by quantitative PCR and RNA sequencing. Metabolic alterations associated with depletion of UGT1A_i2 protein levels stably induced by shRNA (targeting the exon 5b region common to all UGT1A_i2s) were then investigated by complementary approaches including untargeted metabolomics and extracellular flux assays to monitor glycolysis and oxidative phosphorylation. Findings reveal for the first time a significant remodelling of energy metabolism and cellular content of several metabolic intermediates in UGT1A_i2s depleted cancer cells, likely partially explained by a direct interaction with PKM2. These metabolic changes are further associated with a greater migration potential, suggesting that alternate UGT1A proteins might contribute to the oncogenic phenotype of colon cancer cells.

Materials and Method

Immunofluorescence

HT115 cells were obtained from the European Collection of Cell Cultures (Salisbury, UK) and grown as described (Bellemare et al., 2010b). Cells grown on coverslips to 60% confluence were fixed with 4% formaldehyde (Sigma, Oakville, ON, Canada) for 15 min

Molecular Pharmacology Fast Forward. Published on January 3, 2017 as DOI: 10.1124/mol.116.106161
This article has not been copyedited and formatted. The final version may differ from this version.

at room temperature, and permeabilized with 0.5% TX-100 (Sigma) for 5 min. All solutions were prepared in phosphate-buffered saline (PBS). Cells were incubated for 1h30 at RT with primary antibodies diluted in 1% fetal bovine serum (FBS). Primary antibodies were anti-PKM2 (1:500; #3198S, Cell Signaling, Danvers, MA, USA) and the custom mouse monoclonal anti-i2s (1:100; #4C5E7; GenScript, Piscataway, NJ, USA) described in Rouleau et al. (Rouleau et al., 2016). Detection was made with donkey anti-mouse Alexa Fluor 488 (Life Technologies Inc., Burlington, ON, Canada) and goat anti-rabbit Alexa Fluor 594 (Cell Signaling) antibodies on a LSM510 META NLO laser scanning confocal microscope (Zeiss, Toronto, ON, Canada). Images were acquired with the Zen 2009 software (v.5.5 SP1; Zeiss) and were analyzed with ImageJ (v2.0.0; U.S. National Institutes of Health, Bethesda, MD, USA).

Immunoprecipitation and pathway enrichment analysis

Proteomics experiments in commercial pools of human liver and kidney tissues were conducted according to a previous study (Rouleau et al., 2014). Data have been deposited in the PRIDE database under the accession number PXD000295. Briefly, immunoprecipitation was carried out using 1 mg total protein lysate of human liver or kidney S9 fractions (cytosol and microsomes) (Xenotech, Lenexa, KS, USA) with 4 µg anti-UGT1A_i2 #4863 antibody and Protein G–coated magnetic beads (Dynabeads; Life Technologies) for 15 hours at 4°C. Proteins were identified by mass spectrometry using a TripleTOF 5600 after on-beads trypsin digestion. Pathway enrichment analysis was performed with Cytoscape v3.3.0, using ClueGo v2.2.3 and CluePedia v1.2.3 apps (Bindea et al., 2013; Bindea et al., 2009; Shannon et al., 2003). Pathways were retrieved from the KEGG database (updated on January 15, 2016) and an

Molecular Pharmacology Fast Forward. Published on January 3, 2017 as DOI: 10.1124/mol.116.106161
This article has not been copyedited and formatted. The final version may differ from this version.

enrichment/depletion two-sided hypergeometric test with the Bonferroni step down correction method was applied. All presented protein partners were part of a significantly enriched pathway (*q*-value<0.05).

Detection of protein expression and complexes

Co-immunoprecipitations (co-IPs) to confirm partnership with PKM2 were conducted on HT115 cell lysates using the anti-UGT1A_i2s (#4863) and the anti-UGT1A_i1s (#9348) as described (Rouleau et al., 2014). Protein complexes were subjected to SDS-PAGE and detected by Western blotting with UGT1A_i2s (#4863), biotinylated UGT1A_i1 (#9348), and PKM2 (#3198S, Cell Signaling) antibodies. Protein expression was also detected by Western blot. To monitor protein integrity and phosphorylation status,, cells were lysed in Tris buffered solution (175 mM Tris pH 7.4, 150 mM NaCl, 1% Igepal, 1mM DTT) supplemented with Complete protease inhibitor (Roche, Laval, Qc, Canada) and phosSTOP (Sigma). Proteins were revealed using anti-PKM1 (#7067P, Cell Signaling), anti-PKM2 (Cell Signaling), anti-phospho-PKM2 Y105 (#3827; Cell Signaling) and anti-phospho-PKM2 S37 (#11456; Signalway Antibody; College Park, MD, USA). PKM2 dimers and tetramers were crosslinked according to (Wang et al., 2014). Briefly, cell were lysed in PBS (pH 7.4) containing 0.5% Triton X-100 for 30 min, then centrifuged at 16 000 *xg* for 20 min to remove debris. Lysates were then diluted to 4 mg/mL and glutaraldehyde (final concentration 0.0035%) was added to permanently crosslink proteins. After 2 min of incubation at RT, the crosslinking reaction was stopped using Tris pH 8.0 (final concentration 50 mM). Finally, protein complexes were subjected to SDS-PAGE and revealed using anti-PKM2 (Cell Signaling).

Molecular Pharmacology Fast Forward. Published on January 3, 2017 as DOI: 10.1124/mol.116.106161
This article has not been copyedited and formatted. The final version may differ from this version.

Metabolic profiling of HT115 colon cancer cells

Metabolic profiles were established for two HT115 cell lines, a reference HT115 cell line (CTR) and a HT115 cell line in which the expression of UGT1A_i2 proteins were stably repressed (>90%) using a shRNA specific to the exon 5b of *UGT1A* (KD) (Rouleau et al., 2014). Cell lines were grown for a maximum of 15 passages and periodically tested for mycoplasmas. Cells were seeded at 2 x 10^6 cells in a 10 cm petri dish and allowed to adhere and proliferate for four days, with one growth medium change after two days. Cells were trypsinized, centrifuged and counted, before being washed twice with ice-cold PBS and frozen on dry ice. Mass spectrometry analyses were performed by the West Coast Metabolomics Center (UC Davis, Davis, CA, USA) as reported (Fiehn et al., 2010; Fiehn et al., 2008). Data were normalized for cell count and log-transformed prior to testing for statistical differences using two-sided Student's t-tests.

The analysis of extracellular flux was achieved on a Seahorse XF^{e}24 using glycolysis and mitochondria stress kits according to the manufacturer's instructions (Seahorse Bioscience, MA, USA). For the glycolysis stress kit, 100 µL of cells at 2.0 x 10^6 cells/mL were seeded in the dedicated plates, and allowed to adhere for two hours in the incubator before adding 150 µL of pre-warmed culture medium. Cells were grown overnight, rinsed twice with 1 mL Seahorse XF Base Medium (Seahorse Bioscience) supplemented with 4 mM glutamine, and a final volume of 450 µL of the medium was added. Cells were incubated for 1 hour at 37°C and 100% humidity in a non-CO_2 incubator. Test compounds were reconstituted in glutamine-supplemented Seahorse XF Base Medium, according to instructions. A total of 75 µL of this medium was loaded in the injection plate port 'A', while glucose was added in 'B', oligomycin in 'C' and 2-

Molecular Pharmacology Fast Forward. Published on January 3, 2017 as DOI: 10.1124/mol.116.106161
This article has not been copyedited and formatted. The final version may differ from this version.

deoxyglucose in ‘D’. Three measure phases were done for each condition, constituted of three minutes of mixing, two minutes of waiting and three minutes of measuring. For the mitochondria stress kit, a similar protocol was used, except that the Seahorse XF Base Medium was supplemented with both 4 mM glutamine and 4 g/L of glucose, and injection ports were loaded as follows: assay medium in ‘A’, oligomycin in ‘B’, trifluoromethoxy carbonylcyanide phenylhydrazone (FCCP) in ‘C’ and rotenone/antimycin A in ‘D’. Data were normalized for protein content. Number of replicates and independent experiments are specified in the figure legend.

Lactate was quantified with a Lactate Colorimetric/Fluorometric Assay Kit (BioVision, Milpitas, CA, USA). Cells were seeded at 0.6 x 10^6 cells per well in a 6-well plate for 48 hours, rinsed twice with fresh medium and 3 mL of medium was added per well. Medium was sampled at 0, 60, 120 and 180 min and immediately frozen on dry ice. Cells were then trypsinized and counted. A perchloric acid deproteinization kit (BioVision) was used prior to sample dilution and lactate dosage. Fluorescence (Ex/Em = 535/590 nm) was measured on a TECAN M-1000 (Tecan US Inc., Morrisville, NC, USA). Samples were measured in duplicate for each time point. Results represent the mean of two independent experiments and differences were assessed by Student’s two-sided T-tests.

Cellular phenotypes

For proliferation assays, HT115 cells were monitored for 8 days and counted using a TC10 automated cell counter (Bio-Rad, Hercules, California, USA) after addition of Trypan Blue (Sigma). Live cell proliferation assays were conducted on the xCELLigence

Molecular Pharmacology Fast Forward. Published on January 3, 2017 as DOI: 10.1124/mol.116.106161
This article has not been copyedited and formatted. The final version may differ from this version.

DP system according to the manufacturer instructions (ACEA Biosciences Inc., San Diego, CA, USA). Cells were seeded in E-plates (6.0×10^4 cells/well) and monitored every five min for the first four hours, and every 15 min for five days, with the culture medium being changed every 48 hours. In deprivation assays, cells were washed three times with the experimental culture medium before seeding. For glucose deprivation, cells grew in reconstituted glucose free DMEM medium (Sigma), supplemented with 15% FBS (Wisent Bioproducts, St-Bruno, QC, Canada) and 5.6 mM glucose (Sigma). For glutamine deprivation, cells grew in DMEM supplemented with 15% dialyzed FBS and glutamine (Wisent Bioproducts) at a concentration of 0.75 mM or 4 mM. Conditions for serine/glycine deprivation were adapted from (Maddocks et al., 2013). Briefly, MEM medium (Life Technologies) was supplemented with 15% dialyzed FBS, 25 mM glucose (Sigma), 4 mM glutamine and MEM vitamins (Life Technologies). Cells grew either in 0.4 mM serine (Sigma) and glycine (MP Biomedicals, Solon, OH, USA) or in absence of those. Doubling time was calculated with the RTCA Software 2.0 (ACEA Biosciences Inc.), using two points within the exponential proliferation phase. Data are derived from two independent experiments performed at least in triplicate. Differences were assessed with Student's two-sided T-tests.

Adhesion assays were conducted with the ECM 545 adhesion array kit (Millipore Inc., Billerica, MA, USA), according to the manufacturer's instructions. Each well was seeded with 5×10^4 cells in 100 µL of assay buffer. Cells were allowed to adhere for two hours and then rinsed 3 times with the assay buffer. Along with the provided lysis buffer, CyQuant GR DNA dye was added to each well and lysates were transferred in a black plate for fluorescence reading at specified wavelength, i.e. 485 nm (excitation) and

Molecular Pharmacology Fast Forward. Published on January 3, 2017 as DOI: 10.1124/mol.116.106161
This article has not been copyedited and formatted. The final version may differ from this version.

530 nm (emission), on a TECAN M-1000. Data are derived from three independent experiments performed in triplicate and differences were assessed with the two-sided Student's T-tests.

Wound healing assays were conducted using ibidi culture inserts (Minitube Canada, Ingersoll, ON, Canada). Cells were seeded at 9.8 x 10^4 cells/well in a 6-well plate with complete media, and allowed to adhere for 6-8 hours. Cells were then serum-starved overnight and complete media was given 24 hours prior to removal of inserts. Migration was monitored every 24 hours on an inverted Diaphot (Nikon) microscope equipped with a 10X objective and a QICAM (QImaging, Burnaby, BC, Canada) video camera. Five microscopic fields per wound were recorded and the wound area was determined by tracing its contours using ImageJ v1.48. Data are derived from three independent experiments performed in duplicate, and each analyzed independently by two investigators. Differences were assessed with the two-sided Student's T-tests.

mRNA quantification

Human colon tissues (n=6) from primary tumors and paired peritumoral normal tissues were analyzed by reverse transcription and quantitative PCR and are expressed in Relative Quantities (RQ) (Margaillan et al., 2015). RT-qPCR were performed using *UGT1A* specific primers for variants 2/3 (encoding UGT1A_i2s) as described (Bellemare et al., 2010b). Each participant provided written consent, and the local ethic committee approved the study. RNA sequencing data (GSE80463) are from a previous study (Rouleau et al., submitted) and were collected from three pools of colon tissues, each containing total RNA from 5 individuals (normal tissues) or 3 individuals (tumor tissues).

Molecular Pharmacology Fast Forward. Published on January 3, 2017 as DOI: 10.1124/mol.116.106161
This article has not been copyedited and formatted. The final version may differ from this version.

Results

Interaction of UGT1A_i2 proteins with PKM2 in colon cancer HT115 cells

Proteomics experiments in human liver and kidney tissues were conducted according to a previous study (**Fig.1A**). The complete list of identified partners in both tissues is provided (**Supplemental Tables 1 and 2**) based on a previous report (Rouleau et al., 2014). A pathway enrichment analysis of alternate UGT1A_i2 protein partners identified several enzymes linked to pyruvate metabolism, citrate metabolism and glycolysis pathway, including pyruvate kinase involved in glycolysis (**Fig.1B**). We validated the interaction with pyruvate kinase by co-IP in the HT115 cell model that expresses endogenous PKM2, UGT1A_i2s as well as UGT1A_i1 enzymes. These experiments confirmed that PKM2 interacts specifically with the UGT1A_i2 proteins but not with UGT1A_i1 enzymes in HT115 cells (**Fig.1C**). Since PKM2 primarily localized in the cytoplasm (Wang et al., 2014), we then sought to establish the cellular distribution of alternate UGT1A_i2 proteins along with PKM2 **(Fig.1D)**. A subset of UGT1A_i2s co-localized with PKM2 and supports the potential of UGT1A_i2s to interact with PKM2 in this cellular context.

Depletion of UGT1A_i2s enhances glycolytic activity and lactate production but reduces mitochondrial respiration in living colon cancer HT115 cells.

We next assessed the potential influence of UGT1A_i2s on glycolysis and compared HT115 colon cancer cells expressing low (KD) and high (reference or control) UGT1A_i2 levels (**Fig.2A**) (Rouleau et al., 2014). Given that PKM2 and PKM1 expression is similar in both cell models (**Supplemental Fig. 1**), we postulated that the cellular content in

Molecular Pharmacology Fast Forward. Published on January 3, 2017 as DOI: 10.1124/mol.116.106161
This article has not been copyedited and formatted. The final version may differ from this version.

alternate UGT1A_i2s could affect PKM2 activity thereby modifying glucose metabolism to produce lactate, the end product of glycolysis. The accumulation of lactate by 57% (*P*=0.029; **Fig.2B**) in cell medium of KD cells compared to control cells supports a functional impact of UGT1A_i2s on PKM2 activity. We then used an extracellular flux analyzer to measure extracellular acidification rate (ECAR) and oxygen consumption rate (OCR) in living HT115 cells, which reflects glycolytic activity and mitochondrial respiration, respectively. A higher glycolytic activity in the UGT1A_i2s depleted cells was observed as evidenced by a 27% ECAR elevation after addition of glucose to the medium. The maximal glycolytic capacity (measured after addition of oligomycin) was also elevated by 30%, upholding greater utilization of the glycolysis pathway compared to control cells (**Fig.2C,D**). In an assay challenging the mitochondrial capacity and measuring OCR, we detected a lower activity in KD cells supported by lower baseline (-27%) and lower maximal mitochondrial respiration rates (-39%; after addition of FCCP) in these cells compared to control cells (**Fig.2E,F**). Thus, repression of endogenous UGT1A_i2 levels led to higher glycolytic rate at the expense of mitochondrial respiration.

Depletion of UGT1A_i2s induces broad metabolic changes in colon cancer HT115 cells and a greater migration potential.

Given the changes in the energetic pathway induced by depletion of endogenous UGT1A_i2 levels, we extended these studies to global cell metabolism using untargeted metabolomics. A significant effect in the cellular levels of 58 metabolites was observed including many intermediates derived from the glycolysis and TCA cycle pathways. These metabolites include unknown (n=34; data not shown) and known (n=24) metabolites (**Fig.3,4**). Specifically, higher levels of glucose, fructose and citrate were

Molecular Pharmacology Fast Forward. Published on January 3, 2017 as DOI: 10.1124/mol.116.106161
This article has not been copyedited and formatted. The final version may differ from this version.

observed, as well as decreased serine and glutamine cellular contents (**Fig.3B**). Lower levels of several amino acids and some of their metabolites in KD cells were also noted (**Fig.3,4**). These metabolic changes were not associated with differences in cell growth assessed by cell counts, or doubling time determined by a live cell proliferation assay in normal culture conditions or after deprivation of main extracellular carbon sources, glucose and glutamine (**Supplemental Fig.2**). A modest change was noted upon deprivation of the non-essential amino acids serine and glycine (13% longer doubling time; $P<0.05$; **Fig.5A,B**). However, KD cells had a significant greater migration potential (wound closure: 72%; $P<0.05$) compared to control cells (50%) (**Fig.5C-E**). Using an array of extracellular matrix proteins, data further showed a modest but significantly reduced adhesion capacity for KD cells toward collagen I (13%), laminin (10%) and tenascin (11%), compared to control cells (**Fig.5F**).

Downregulation of UGT1A_i2s mRNA expression in colon tumors compared to normal tissues

To evaluate the potential relevance of our observations using the HT115 model in which endogenous UGT1A_i2 levels were depleted, we studied UGT1A_i2s expression in colon tumors compared to normal tissues. Quantitative PCR expression of the alternative mRNA variants (*v2/v3)* encoding UGT1A_i2 proteins assessed in primary colon tumors and paired peritumoral normal tissues revealed that most tumors (4/6; 67%) had a reduced UGT1A_i2s expression compared to normal tissues (**Fig.6A**). This observation was further confirmed using RNA sequencing data generated from an independent set of colon samples (Fold change = -20.5; $P<0.05$; **Fig.6B**).

Molecular Pharmacology Fast Forward. Published on January 3, 2017 as DOI: 10.1124/mol.116.106161
This article has not been copyedited and formatted. The final version may differ from this version.

Discussion

It is now well established that there is a strong and multifaceted connection between cell metabolism and cancer (Li and Zhang, 2016; Vander Heiden et al., 2009), while alternative splice variants of many cancer-related genes directly contribute to the oncogenic phenotype (Oltean and Bates, 2014). We showed that depletion of UGT1A_i2 proteins in the colon cancer cell model HT115 enforces the Warburg effect, modifies levels of cellular metabolic intermediates and impacts migration properties. These metabolic and phenotypic changes may be explained, at least in part, by the interaction between UGT1A_i2s and PKM2, a key enzyme of the glycolysis pathway. Since glycolysis-related pathways determine cellular energy level, redox homeostasis and ability to proliferate (Vander Heiden et al., 2011), it is plausible that alternate UGT1A_i2 proteins play a role in oncogenic phenotypes. In support, the metabolic adaptation of cancer cells, which oxidize carbohydrates at a reduced rate even in the presence of oxygen, was shown to be greater in the absence of UGT1A_i2 proteins, suggesting a functional role of its interaction with the glycolytic enzyme PKM2. The production of excess amounts of lactate released from cancer cells also supports this notion. The *in vivo* relevance of our observations was further supported by a severely decreased UGT1A_i2s expression in colon tumors compared to normal tissues established by quantitative PCR and RNA sequencing, and in few specimens by IHC (Bellemare et al., 2011), in line with a potential role of alternate UGT1A proteins in tumor cell biology.

Previous studies have linked energy metabolism to colon cancer progression, and as a rate-limiting enzyme of glycolysis, PKM2 has been investigated (Li et al., 2014; Lunt et al., 2015; Yang et al., 2014; Zhou et al., 2012). Zhou et al (Zhou et al., 2012) have

Molecular Pharmacology Fast Forward. Published on January 3, 2017 as DOI: 10.1124/mol.116.106161
This article has not been copyedited and formatted. The final version may differ from this version.

reported an upregulation of PKM2 in colorectal cancer, and that its knockdown suppressed the proliferation and migration of colon cancer RKO cells. Other findings indicated that the activity of PKM2 is pivotal for the fate of pyruvate: the highly active PKM2 tetramer (high pyruvate kinase activity) leads to pyruvate oxidation in the TCA cycle, whereas the less active PKM2 dimer (low pyruvate kinase activity) enhances the conversion of pyruvate into lactate by the lactate dehydrogenase and favors synthesis of cell constituents (Anastasiou et al., 2012; Christofk et al., 2008a). Our analysis of extracellular flux in real-time uncovered an enhanced glycolytic activity and a lower OXPHOS capacity for KD cells, which is in accordance with a rerouting of carbohydrates toward lactate instead of TCA cycle. We also observed accumulation of lactate in KD cell medium, further suggesting that the presence of UGT1A_i2 proteins interferes with the glycolytic pathway. Given that PKM2 and PKM1 expression is similar in both cell models (**Supplemental Fig. 1A**), we investigated the status of PKM2 phosphorylation and oligomerization. Phosphorylation of PKM2 at position Y_{105}, favoring lactate production by the less active dimeric PKM2 conformation, was slightly enhanced in KD relative to control cells (**Supplemental Fig.1A**) whereas the PKM2 tetramer/dimer ratios were similar between the two model cell lines, unsupportive of a modulation of PKM2 oligomeric state by UGT1A_i2s (**Supplemental Fig.1B**). PKM2 may also be involved in other functions in tumorigenesis and metastasis, since PKM2 was shown to act in the nucleus by regulating gene expression (Wang et al., 2014; Yang et al., 2012). However, our previous analysis of global gene expression in HT115 cell lines suggest that the KD of UGT1A_i2s does not induce significant perturbations in gene expression of glycolytic enzymes or of other metabolic pathways, including genes modulated by PKM2 and

Molecular Pharmacology Fast Forward. Published on January 3, 2017 as DOI: 10.1124/mol.116.106161
This article has not been copyedited and formatted. The final version may differ from this version.

reported to modulate migration and epithelial-mesenchymal transition (Hamabe et al., 2014; Rouleau et al., 2014; Yang et al., 2014). Consistently, levels of phospho-PKM2 (position S_{37}) involved in nuclear translocation and functions of PKM2, were not altered by a KD of UGT1A_i2s (**Supplemental Fig.1**). Therefore, it may be envisioned that the interaction between PKM2 and alternate UGT1A_i2 proteins might influence PKM2 allosteric regulation. In line with this notion, similar functional interactions of PKM2 with other proteins such as the promyelocytic leukemia (PML) tumor suppressor protein, the prolactin receptor, and the phosphoprotein (pp60src)-associated protein kinase of Rous sarcoma virus led to reduced pyruvate kinase activity through allosteric regulation (Christofk et al., 2008b; Gao et al., 2013; Glossmann et al., 1981; Mazurek et al., 2001; Presek et al., 1980; Shimada et al., 2008; Varghese et al., 2010). Whether this could be mediated by direct interactions with phosphorylated UGT1A_i2s *(Basu et al., 2003; Basu et al., 2005; Volak and Court, 2010)* or by a UGT1A_i2-dependent modulation of interactions between PKM2 and other allosteric modulators will necessitate additional investigations. From a therapeutic perspective PKM2 expression and activity can be regulated by inhibitors and activators that have been tested *in vitro* and *in vivo* (Dong et al., 2016).

The greater migration potential provoked by UGT1A_i2s KD in HT115 cells is in line with a shift from oxidative metabolism to aerobic glycolysis reported in more aggressive colon cancer cells (Hussain et al., 2016). Consistent with our observation that lactate accumulates in the medium of UGT1A_i2s KD compared to control cells; this oncometabolite was shown to act not only as a potent fuel (oxidative) but also function as a signalling molecule to stimulate tumor angiogenesis (Doherty and Cleveland,

Molecular Pharmacology Fast Forward. Published on January 3, 2017 as DOI: 10.1124/mol.116.106161
This article has not been copyedited and formatted. The final version may differ from this version.

2013). Moreover, the mitochondrial oxidative metabolism is viewed as a critical suppressor of metastasis and thus, lower OXPHOS activity may help promote metastasis (Lu et al., 2015). Cell migration is an early requirement for tumor metastasis (Findlay et al., 2014), but is a complex phenomenon that involves cycling of adhesion and cell detachment (Kurniawan et al., 2016; Pankova et al., 2010; Tozluoglu et al., 2013). Strongly adherent cells may increase their migration capacity through a decrease of their adhesion to extracellular matrix. While subtle, we observed a differential adhesion capacity of KD cells, namely for laminin, a non-collagenous extracellular matrix critical in colon cancer and linked to tumor angiogenesis, epithelial-mesenchymal transition and metastasis (Guess et al., 2009; Kitayama et al., 1999; Simon-Assmann et al., 2011). Accordingly, this observation may partially explain the differential migration phenotype between low and high UGT1A_i2 expressing cell lines.

A potential limitation is the fact that metabolomics data were derived from a single time-point, and thus represent the sum of numerous metabolic reactions that occurred in a 48-hour period. The cellular content of several metabolic intermediates from the glycolysis and TCA cycle pathways was changed in UGT1A_i2-depleted HT115 cells compared to control cells and are unlikely explained solely by the protein-protein interaction between UGT1A_i2s and PKM2. Additional partnerships observed by proteomics, such as those with enzymes of the gluconeogenesis and TCA cycle that require additional validation by co-IP, may also underlie these observations. Of note, data revealed a globally reduced pool of glucogenic amino acids in KD cells. This is consistent with the enhanced glycolytic potential induced by the KD and with the identification of additional i2 protein partners associated with gluconeogenesis, for

Molecular Pharmacology Fast Forward. Published on January 3, 2017 as DOI: 10.1124/mol.116.106161
This article has not been copyedited and formatted. The final version may differ from this version.

instance pyruvate carboxylase (PC) and phosphoenolpyruvate carboxykinase (PCK1 and PCK2). Furthermore, the lower serine levels in KD cells compared to CTR suggested that the *de novo* serine synthesis pathway, critical for cancer cell proliferation and metabolism (Mehrmohamadi and Locasale, 2015; Yoon et al., 2015), might be perturbed. We thus expected that serine and glycine deprivation would increase the metabolic pressure on glycolysis through a deviation of its intermediates. Although modest, a significantly decreased cellular proliferation for KD cells was observed in these conditions, compared to control cells. It remains unknown whether a specific UGT1A_i2 protein or several of those expressed in the HT115 cell model trigger the observed effects given that all UGT1A_i2s were simultaneously repressed by shRNA. Additional cell models need to be established to further investigate our initial findings.

To the best of our knowledge, this is the first identification of a functional link between the UGT pathway and energy metabolism implying that alternate UGT1A proteins might be regulators of PKM2 with consequences on cancer cell metabolism and phenotype. It may be unexpected that a depletion of alternate UGT1A_i2s is sufficient to alter the metabolic program of colon cancer cells given the numerous, redundant, and efficacious mechanisms in place to limit pyruvate oxidation in cancer cells. In the face of these counteracting mechanisms, the metabolic effects of UGT1A_i2s depletion are rather impressive and may be explained in part by an interaction with the key glycolytic and multifunctional enzyme PKM2, and most likely with other metabolic enzymes. Although there was no change in UDPGlcA cell content between the two cell models, another possibility could involve the allosteric modulation by UDPGlcA and/or other UDP-sugars, as reported for other glycolytic enzymes (Wu et al., 2006). It also remains to be

Molecular Pharmacology Fast Forward. Published on January 3, 2017 as DOI: 10.1124/mol.116.106161
This article has not been copyedited and formatted. The final version may differ from this version.

demonstrated whether UGT1A_i2s possess enzyme activity by utilizing other UDP-sugars for instance. Alternatively, the effects observed on metabolism could be mediated through an impact on endogenous levels of key metabolic molecules that are unknown substrates of UGT enzymes repressed by UGT1A_i2s. Findings thus support that alternate UGT1A proteins are potential metabolic regulators of cancer cell metabolism and that they may contribute to the oncogenic phenotype of colon cancer cells. We conclude that alternate UGT proteins may be part of the expanding compendium of metabolic pathways involved in cancer biology. However, further investigations of UGT1A alternate proteins in cancer metabolism are required, as the crosstalk between global cell metabolism and the UGT pathway may likely constitute a key vulnerability in cancer cells that could be exploited.

Conflict of interest: The authors have declared that no conflict of interest exists.

Acknowledgments

We would like to acknowledge Lyne Villeneuve, Andréa Fournier, Patrick Caron and Véronique Turcotte for technical support. We acknowledge the support from Michèle Orain for help with handling of human tissues.

Molecular Pharmacology Fast Forward. Published on January 3, 2017 as DOI: 10.1124/mol.116.106161
This article has not been copyedited and formatted. The final version may differ from this version.

Authorship contributions

Participated in research design: Mi Rouleau, Guillemette

Conducted experiments: Audet-Delage, Me Rouleau, Roberge

Contributed new reagents or analytic tools: Miard, Picard, Têtu

Performed data analysis: Audet-Delage, Mi Rouleau, Me Rouleau, Roberge, Miard, Guillemette

Wrote or contributed to the writing of the manuscript: Audet-Delage, Mi Rouleau, Me Rouleau, Guillemette

Molecular Pharmacology Fast Forward. Published on January 3, 2017 as DOI: 10.1124/mol.116.106161
This article has not been copyedited and formatted. The final version may differ from this version.

References

Anastasiou D, Yu Y, Israelsen WJ, Jiang JK, Boxer MB, Hong BS, Tempel W, Dimov S, Shen M, Jha A, Yang H, Mattaini KR, Metallo CM, Fiske BP, Courtney KD, Malstrom S, Khan TM, Kung C, Skoumbourdis AP, Veith H, Southall N, Walsh MJ, Brimacombe KR, Leister W, Lunt SY, Johnson ZR, Yen KE, Kunii K, Davidson SM, Christofk HR, Austin CP, Inglese J, Harris MH, Asara JM, Stephanopoulos G, Salituro FG, Jin S, Dang L, Auld DS, Park HW, Cantley LC, Thomas CJ and Vander Heiden MG (2012) Pyruvate kinase M2 activators promote tetramer formation and suppress tumorigenesis. *Nat Chem Biol* **8**: 839-847.

Basu NK, Kole L and Owens IS (2003) Evidence for phosphorylation requirement for human bilirubin UDP-glucuronosyltransferase (UGT1A1) activity. *Biochem Biophys Res Commun* **303**: 98-104.

Basu NK, Kovarova M, Garza A, Kubota S, Saha T, Mitra PS, Banerjee R, Rivera J and Owens IS (2005) Phosphorylation of a UDP-glucuronosyltransferase regulates substrate specificity. *Proc Natl Acad Sci U S A* **102**: 6285-6290.

Bellemare J, Rouleau M, Girard H, Harvey M and Guillemette C (2010a) Alternatively spliced products of the UGT1A gene interact with the enzymatically active proteins to inhibit glucuronosyltransferase activity in vitro. *Drug Metab Dispos* **38**: 1785-1789.

Bellemare J, Rouleau M, Harvey M, Popa I, Pelletier G, Tetu B and Guillemette C (2011) Immunohistochemical expression of conjugating UGT1A-derived isoforms in normal and tumoral drug-metabolizing tissues in humans. *J Pathol* **223**: 425-435.

Molecular Pharmacology Fast Forward. Published on January 3, 2017 as DOI: 10.1124/mol.116.106161
This article has not been copyedited and formatted. The final version may differ from this version.

Bellemare J, Rouleau M, Harvey M, Tetu B and Guillemette C (2010b) Alternative-splicing forms of the major phase II conjugating UGT1A gene negatively regulate glucuronidation in human carcinoma cell lines. *Pharmacogenomics J* **10**: 431-441.

Biamonti G, Catillo M, Pignataro D, Montecucco A and Ghigna C (2014) The alternative splicing side of cancer. *Semin Cell Dev Biol* **32**: 30-36.

Bindea G, Galon J and Mlecnik B (2013) CluePedia Cytoscape plugin: pathway insights using integrated experimental and in silico data. *Bioinformatics* **29**: 661-663.

Bindea G, Mlecnik B, Hackl H, Charoentong P, Tosolini M, Kirilovsky A, Fridman WH, Pages F, Trajanoski Z and Galon J (2009) ClueGO: a Cytoscape plug-in to decipher functionally grouped gene ontology and pathway annotation networks. *Bioinformatics* **25**: 1091-1093.

Bluemlein K, Gruning NM, Feichtinger RG, Lehrach H, Kofler B and Ralser M (2011) No evidence for a shift in pyruvate kinase PKM1 to PKM2 expression during tumorigenesis. *Oncotarget* **2**: 393-400.

Christofk HR, Vander Heiden MG, Harris MH, Ramanathan A, Gerszten RE, Wei R, Fleming MD, Schreiber SL and Cantley LC (2008a) The M2 splice isoform of pyruvate kinase is important for cancer metabolism and tumour growth. *Nature* **452**: 230-233.

Christofk HR, Vander Heiden MG, Wu N, Asara JM and Cantley LC (2008b) Pyruvate kinase M2 is a phosphotyrosine-binding protein. *Nature* **452**: 181-186.

Cui R and Shi XY (2015) Expression of pyruvate kinase M2 in human colorectal cancer and its prognostic value. *Int J Clin Exp Pathol* **8**: 11393-11399.

Doherty JR and Cleveland JL (2013) Targeting lactate metabolism for cancer therapeutics. *J Clin Invest* **123**: 3685-3692.

Dong G, Mao Q, Xia W, Xu Y, Wang J, Xu L and Jiang F (2016) PKM2 and cancer: The function of PKM2 beyond glycolysis. *Oncol Lett* **11**: 1980-1986.

Fiehn O, Garvey WT, Newman JW, Lok KH, Hoppel CL and Adams SH (2010) Plasma metabolomic profiles reflective of glucose homeostasis in non-diabetic and type 2 diabetic obese African-American women. *PLoS One* **5**: e15234.

Fiehn O, Wohlgemuth G, Scholz M, Kind T, Lee DY, Lu Y, Moon S and Nikolau B (2008) Quality control for plant metabolomics: reporting MSI-compliant studies. *Plant J* **53**: 691-704.

Findlay VJ, Wang C, Watson DK and Camp ER (2014) Epithelial-to-mesenchymal transition and the cancer stem cell phenotype: insights from cancer biology with therapeutic implications for colorectal cancer. *Cancer Gene Ther* **21**: 181-187.

Gao X, Wang H, Yang JJ, Chen J, Jie J, Li L, Zhang Y and Liu ZR (2013) Reciprocal regulation of protein kinase and pyruvate kinase activities of pyruvate kinase M2 by growth signals. *J Biol Chem* **288**: 15971-15979.

Girard H, Levesque E, Bellemare J, Journault K, Caillier B and Guillemette C (2007) Genetic diversity at the UGT1 locus is amplified by a novel 3' alternative splicing mechanism leading to nine additional UGT1A proteins that act as regulators of glucuronidation activity. *Pharmacogenet Genomics* **17**: 1077-1089.

Glossmann H, Presek P and Eigenbrodt E (1981) Association of the src-gene product of Rous sarcoma virus with a pyruvate-kinase inactivation factor. *Mol Cell Endocrinol* **23**: 49-63.

Guess CM, Lafleur BJ, Weidow BL and Quaranta V (2009) A decreased ratio of laminin-332 beta3 to gamma2 subunit mRNA is associated with poor prognosis in colon cancer. *Cancer Epidemiol Biomarkers Prev* **18**: 1584-1590.

Gupta V and Bamezai RN (2010) Human pyruvate kinase M2: a multifunctional protein. *Protein Sci* **19**: 2031-2044.

Hamabe A, Konno M, Tanuma N, Shima H, Tsunekuni K, Kawamoto K, Nishida N, Koseki J, Mimori K, Gotoh N, Yamamoto H, Doki Y, Mori M and Ishii H (2014) Role of pyruvate kinase M2 in transcriptional regulation leading to epithelial-mesenchymal transition. *Proc Natl Acad Sci U S A* **111**: 15526-15531.

Hussain A, Qazi AK, Mupparapu N, Guru SK, Kumar A, Sharma PR, Singh SK, Singh P, Dar MJ, Bharate SB, Zargar MA, Ahmed QN, Bhushan S, Vishwakarma RA and Hamid A (2016) Modulation of glycolysis and lipogenesis by novel PI3K selective molecule represses tumor angiogenesis and decreases colorectal cancer growth. *Cancer Lett* **374**: 250-260.

Israelsen WJ and Vander Heiden MG (2015) Pyruvate kinase: Function, regulation and role in cancer. *Semin Cell Dev Biol* **43**: 43-51.

Kitayama J, Nagawa H, Tsuno N, Osada T, Hatano K, Sunami E, Saito H and Muto T (1999) Laminin mediates tethering and spreading of colon cancer cells in physiological shear flow. *Br J Cancer* **80**: 1927-1934.

Kurniawan NA, Chaudhuri PK and Lim CT (2016) Mechanobiology of cell migration in the context of dynamic two-way cell-matrix interactions. *J Biomech* **49**: 1355-1368.

Molecular Pharmacology Fast Forward. Published on January 3, 2017 as DOI: 10.1124/mol.116.106161
This article has not been copyedited and formatted. The final version may differ from this version.

Levesque E, Girard H, Journault K, Lepine J and Guillemette C (2007) Regulation of the UGT1A1 bilirubin-conjugating pathway: role of a new splicing event at the UGT1A locus. *Hepatology* **45**: 128-138.

Li L, Zhang Y, Qiao J, Yang JJ and Liu ZR (2014) Pyruvate kinase M2 in blood circulation facilitates tumor growth by promoting angiogenesis. *J Biol Chem* **289**: 25812-25821.

Li Z and Zhang H (2016) Reprogramming of glucose, fatty acid and amino acid metabolism for cancer progression. *Cell Mol Life Sci* **73**: 377-392.

Lu J, Tan M and Cai Q (2015) The Warburg effect in tumor progression: mitochondrial oxidative metabolism as an anti-metastasis mechanism. *Cancer Lett* **356**: 156-164.

Lunt SY, Muralidhar V, Hosios AM, Israelsen WJ, Gui DY, Newhouse L, Ogrodzinski M, Hecht V, Xu K, Acevedo PN, Hollern DP, Bellinger G, Dayton TL, Christen S, Elia I, Dinh AT, Stephanopoulos G, Manalis SR, Yaffe MB, Andrechek ER, Fendt SM and Vander Heiden MG (2015) Pyruvate kinase isoform expression alters nucleotide synthesis to impact cell proliferation. *Mol Cell* **57**: 95-107.

Maddocks OD, Berkers CR, Mason SM, Zheng L, Blyth K, Gottlieb E and Vousden KH (2013) Serine starvation induces stress and p53-dependent metabolic remodelling in cancer cells. *Nature* **493**: 542-546.

Margaillan G, Rouleau M, Fallon JK, Caron P, Villeneuve L, Turcotte V, Smith PC, Joy MS and Guillemette C (2015) Quantitative profiling of human renal UDP-glucuronosyltransferases and glucuronidation activity: a comparison of normal and tumoral kidney tissues. *Drug Metab Dispos* **43**: 611-619.

Mazurek S, Zwerschke W, Jansen-Durr P and Eigenbrodt E (2001) Metabolic cooperation between different oncogenes during cell transformation: interaction between activated ras and HPV-16 E7. *Oncogene* **20**: 6891-6898.

Mehrmohamadi M and Locasale JW (2015) Context dependent utilization of serine in cancer. *Mol Cell Oncol* **2**: e996418.

Mitsopoulos C, Schierz AC, Workman P and Al-Lazikani B (2015) Distinctive Behaviors of Druggable Proteins in Cellular Networks. *PLoS Comput Biol* **11**: e1004597.

Miyauchi Y, Nagata K, Yamazoe Y, Mackenzie PI, Yamada H and Ishii Y (2015) Suppression of Cytochrome P450 3A4 Function by UDP-Glucuronosyltransferase 2B7 through a Protein-Protein Interaction: Cooperative Roles of the Cytosolic Carboxyl-Terminal Domain and the Luminal Anchoring Region. *Mol Pharmacol* **88**: 800-812.

Oltean S and Bates DO (2014) Hallmarks of alternative splicing in cancer. *Oncogene* **33**: 5311-5318.

Pankova K, Rosel D, Novotny M and Brabek J (2010) The molecular mechanisms of transition between mesenchymal and amoeboid invasiveness in tumor cells. *Cell Mol Life Sci* **67**: 63-71.

Presek P, Glossmann H, Eigenbrodt E, Schoner W, Rubsamen H, Friis RR and Bauer H (1980) Similarities between a phosphoprotein (pp60src)-associated protein kinase of Rous sarcoma virus and a cyclic adenosine 3':5'-monophosphate-independent protein kinase that phosphorylates pyruvate kinase type M2. *Cancer Res* **40**: 1733-1741.

Rouleau M, Roberge J, Bellemare J and Guillemette C (2014) Dual roles for splice variants of the glucuronidation pathway as regulators of cellular metabolism. *Mol Pharmacol* **85**: 29-36.

Rouleau M, Tourancheau A, Girard-Bock C, Villeneuve L, Vaucher J, Duperre AM, Audet-Delage Y, Gilbert I, Popa I, Droit A and Guillemette C (2016) Divergent Expression and Metabolic Functions of Human Glucuronosyltransferases through Alternative Splicing. *Cell reports* **17**: 114-124.

Rowland A, Miners JO and Mackenzie PI (2013) The UDP-glucuronosyltransferases: their role in drug metabolism and detoxification. *Int J Biochem Cell Biol* **45**: 1121-1132.

Scott DE, Bayly AR, Abell C and Skidmore J (2016) Small molecules, big targets: drug discovery faces the protein-protein interaction challenge. *Nat Rev Drug Discov* **15**: 533-550.

Shannon P, Markiel A, Ozier O, Baliga NS, Wang JT, Ramage D, Amin N, Schwikowski B and Ideker T (2003) Cytoscape: a software environment for integrated models of biomolecular interaction networks. *Genome Res* **13**: 2498-2504.

Shimada N, Shinagawa T and Ishii S (2008) Modulation of M2-type pyruvate kinase activity by the cytoplasmic PML tumor suppressor protein. *Genes Cells* **13**: 245-254.

Simon-Assmann P, Orend G, Mammadova-Bach E, Spenle C and Lefebvre O (2011) Role of laminins in physiological and pathological angiogenesis. *Int J Dev Biol* **55**: 455-465.

Stingl JC, Bartels H, Viviani R, Lehmann ML and Brockmoller J (2014) Relevance of UDP-glucuronosyltransferase polymorphisms for drug dosing: A quantitative systematic review. *Pharmacol Ther* **141**: 92-116.

Taniguchi K, Ito Y, Sugito N, Kumazaki M, Shinohara H, Yamada N, Nakagawa Y, Sugiyama T, Futamura M, Otsuki Y, Yoshida K, Uchiyama K and Akao Y (2015) Organ-specific PTB1-associated microRNAs determine expression of pyruvate kinase isoforms. *Sci Rep* **5**: 8647.

Tozluoglu M, Tournier AL, Jenkins RP, Hooper S, Bates PA and Sahai E (2013) Matrix geometry determines optimal cancer cell migration strategy and modulates response to interventions. *Nat Cell Biol* **15**: 751-762.

Vander Heiden MG, Cantley LC and Thompson CB (2009) Understanding the Warburg effect: the metabolic requirements of cell proliferation. *Science* **324**: 1029-1033.

Vander Heiden MG, Lunt SY, Dayton TL, Fiske BP, Israelsen WJ, Mattaini KR, Vokes NI, Stephanopoulos G, Cantley LC, Metallo CM and Locasale JW (2011) Metabolic pathway alterations that support cell proliferation. *Cold Spring Harb Symp Quant Biol* **76**: 325-334.

Varghese B, Swaminathan G, Plotnikov A, Tzimas C, Yang N, Rui H and Fuchs SY (2010) Prolactin inhibits activity of pyruvate kinase M2 to stimulate cell proliferation. *Mol Endocrinol* **24**: 2356-2365.

Volak LP and Court MH (2010) Role for protein kinase C delta in the functional activity of human UGT1A6: implications for drug-drug interactions between PKC inhibitors and UGT1A6. *Xenobiotica* **40**: 306-318.

Wang HJ, Hsieh YJ, Cheng WC, Lin CP, Lin YS, Yang SF, Chen CC, Izumiya Y, Yu JS, Kung HJ and Wang WC (2014) JMJD5 regulates PKM2 nuclear translocation and reprograms HIF-1alpha-mediated glucose metabolism. *Proc Natl Acad Sci U S A* **111**: 279-284.

Warburg O, Wind F and Negelein E (1927) The Metabolism of Tumors in the Body. *J Gen Physiol* **8**: 519-530.

Wu C, Khan SA, Peng LJ and Lange AJ (2006) Roles for fructose-2,6-bisphosphate in the control of fuel metabolism: beyond its allosteric effects on glycolytic and gluconeogenic enzymes. *Advances in enzyme regulation* **46**: 72-88.

Yang P, Li Z, Fu R, Wu H and Li Z (2014) Pyruvate kinase M2 facilitates colon cancer cell migration via the modulation of STAT3 signalling. *Cell Signal* **26**: 1853-1862.

Yang P, Li Z, Wang Y, Zhang L, Wu H and Li Z (2015) Secreted pyruvate kinase M2 facilitates cell migration via PI3K/Akt and Wnt/beta-catenin pathway in colon cancer cells. *Biochem Biophys Res Commun* **459**: 327-332.

Yang W, Zheng Y, Xia Y, Ji H, Chen X, Guo F, Lyssiotis CA, Aldape K, Cantley LC and Lu Z (2012) ERK1/2-dependent phosphorylation and nuclear translocation of PKM2 promotes the Warburg effect. *Nat Cell Biol* **14**: 1295-1304.

Yang X, Coulombe-Huntington J, Kang S, Sheynkman GM, Hao T, Richardson A, Sun S, Yang F, Shen YA, Murray RR, Spirohn K, Begg BE, Duran-Frigola M, MacWilliams A, Pevzner SJ, Zhong Q, Trigg SA, Tam S, Ghamsari L, Sahni N, Yi S, Rodriguez MD, Balcha D, Tan G, Costanzo M, Andrews B, Boone C, Zhou XJ, Salehi-Ashtiani K, Charloteaux B, Chen AA, Calderwood MA, Aloy P, Roth FP,

Molecular Pharmacology Fast Forward. Published on January 3, 2017 as DOI: 10.1124/mol.116.106161
This article has not been copyedited and formatted. The final version may differ from this version.

Hill DE, Iakoucheva LM, Xia Y and Vidal M (2016) Widespread Expansion of Protein Interaction Capabilities by Alternative Splicing. *Cell* **164**: 805-817.

Yoon S, Kim JG, Seo AN, Park SY, Kim HJ, Park JS, Choi GS, Jeong JY, Jun do Y, Yoon GS and Kang BW (2015) Clinical Implication of Serine Metabolism-Associated Enzymes in Colon Cancer. *Oncology* **89**: 351-359.

Zhan C, Yan L, Wang L, Ma J, Jiang W, Zhang Y, Shi Y and Wang Q (2015) Isoform switch of pyruvate kinase M1 indeed occurs but not to pyruvate kinase M2 in human tumorigenesis. *PLoS One* **10**: e0118663.

Zhou CF, Li XB, Sun H, Zhang B, Han YS, Jiang Y, Zhuang QL, Fang J and Wu GH (2012) Pyruvate kinase type M2 is upregulated in colorectal cancer and promotes proliferation and migration of colon cancer cells. *IUBMB Life* **64**: 775-782.

Molecular Pharmacology Fast Forward. Published on January 3, 2017 as DOI: 10.1124/mol.116.106161
This article has not been copyedited and formatted. The final version may differ from this version.

Figures legends

Figure 1. Interaction between UGT1A_i2s and energy metabolism-related proteins. **A)** Experimental scheme of the affinity purification/mass spectrometry identification of UGT1A_i2 endogenous protein partners. Peptide coordinates are those of UGT1A1. **B)** Pathway enrichment analysis, according to KEGG, of proteins immunprecipitated with UGT1A_i2s. Main metabolic pathways are 'Citrate Cycle (TCA cycle)' and 'Tryptophan Metabolism'. Enriched pathways related to TCA cycle (kappa>0.4) through protein sharing are indicated by blue circles. Circle sizes are proportional to the number of proteins identified within each pathway. A selection of significantly enriched pathways (*q*-value<0.05) and their proteins is shown. **C)** PKM2 endogenously interacts with UGT1A_i2 alternate proteins in HT115 cells, but not with UGT1A_i1 enzymes. Immunoprecipitation (IP) was carried out from a whole HT115 cell lysate (HT115) and revealed by western blotting (WB) using antibodies specific to indicated proteins. **D)** UGT1A_i2 alternate proteins co-localize with PKM2 in HT115 cells. Fluorescence intensity profiles are given for the cross-section (dashed line in the merge panel). The scale bar represents 5 µm.

Figure 2. Remodelling of the energy metabolism in UGT1A_i2s depleted HT115 (KD) cells compared to control (CTR) cells. A) HT115 colon cancer cell models. UGT1A_i2s expression is stably depleted (KD) by a shRNA specific to exon 5b. Control cells (CTR) carry a non-targeting shRNA. Upper panel: Depletion of i2s does not affect i1 enzymes expression. Lower panel: i2s are depleted by 90% in KD cells. Multiple protein bands reflect expression of several of the nine UGT1A_i2 proteins in HT115 cells. First two lanes: lysates from HEK293 cells (UGT negative) overexpressing i1 and

Molecular Pharmacology Fast Forward. Published on January 3, 2017 as DOI: 10.1124/mol.116.106161
This article has not been copyedited and formatted. The final version may differ from this version.

i2 demonstrate specificity of anti-UGT1A_i1s (#9348) and anti-UGT1A_i2s (#4C5E7). **B)** Lactate formation in growth medium of HT115 cells over time, corrected for baseline and normalized by cell count. Data (mean ± SD) are derived from at least two independent experiments performed in duplicate. **C)** Glycolytic profile of KD cells. Extracellular acidification rates (ECAR) were measured by extracellular flux using the glycolysis stress kit. Representative profiles from three independent experiments performed in triplicate are shown. Injection of compounds during the assay is highlighted. **D)** Relative glycolytic and maximal glycolytic capacity, extracted from time points with the highest response, during the glycolysis stress assay, to glucose and oligomycin, respectively. Data (mean ± SD) are derived from three independent experiments performed in triplicate and were normalized for protein concentration. **E)** Mitochondrial respiration profile of KD cells. Oxygen consumption rates (OCR) were measured by extracellular flux using the mitochondria stress kit. Representative profiles from three independent experiments performed in triplicate. Injection of compounds during the assay is highlighted. **F)** Relative basal and maximal mitochondrial respiration, extracted from the last basal time point and the time point with the highest response to FCCP during the mitochondria stress assay, respectively. Data (mean ± SD) are derived from three independent experiments performed in triplicate and were normalized for protein concentration. * $P<0.05$; ** $P<0.01$; *** $P<0.001$.

Figure 3. Untargeted metabolomics analysis of UGT1A_i2s-depleted HT115 cells (KD) and control (CTR) cells. A) Cellular levels of known metabolites (n=144) are shown. Dotted lines represent a 20% fold change (FC). **B)** Known metabolites (n=24) significantly altered in HT115 KD cells compared to control cells.

Molecular Pharmacology Fast Forward. Published on January 3, 2017 as DOI: 10.1124/mol.116.106161
This article has not been copyedited and formatted. The final version may differ from this version.

Figure 4. Depletion of UGT1A_i2s perturbs glycolysis, TCA cycle and amino acids. Relative levels (arbitrary units) of selected metabolites in HT115 CTR and KD cells are given in the context of bioenergetic pathways. Glucose-6-Phosphate (G-6-P), Fructose-6-P (F-6-P), Fructose1-6-Bisphosphate (F-1-6-BP), Glyceraldehyde-3-Phosphate (GA-3-P), Glyceraldehyde (GA), Fructose-1-Phosphate (F-1-P), Dihydroxyacetone phosphate (DHAP), Glycerate-3-Phosphate (G-3-P), Phosphoenolpyruvate (PEP), 2-oxoglutarate (2-OG). The pink background highlights the TCA cycle and the blue background highlights amino acids. CTR: control cells; KD: UGT1A_i2s-depleted cells. Data normalized for cell count. * $P<0.05$; ** $P<0.01$.

Figure 5. Proliferation, migration and adhesion of HT115 cells. A) Live-cell proliferation assay of HT115 cell models with or without deprivation of serine (S) and glycine (G), as detected by an impedance-based system. Graph of a representative experiment is shown. **B)** Doubling time ratio between growth with S/G (dark bars) and without S/G (light bars) for each cell line. Data represent values of 2 independent experiments. Proliferation data in basal conditions and with glucose or glutamine deprivation are shown in Supplemental Fig. 2. **C)** HT115 UGT1A_i2s-depleted cells (KD) have an increased migration potential. Representative images of cells in a wound healing assay at wound induction (t_0) and 24 hrs post-wounding (t_{24}). Image enlargement: 10X. **D)** Wound area (arbitrary units) of images shown in C were measured using ImageJ. **E)** Relative wound closure was calculated from three wound healing assays performed in triplicate and analyzed independently by two investigators. **F)** Decreased adhesion of HT115 KD cells relative to CTR. An extracellular matrix assay detected a lower adhesion profile for Collagen I (Col I), Laminin (Lam) and Tenascin

Molecular Pharmacology Fast Forward. Published on January 3, 2017 as DOI: 10.1124/mol.116.106161
This article has not been copyedited and formatted. The final version may differ from this version.

(Ten) in KD cells. Other matrices: Collagen II (Col II); Collagen IV (Col IV); Fibronectin (Fibro); Vitronectin (Vitro); and Bovine Serum Albumin (BSA, as negative control). Mean ± SEM. n=3 independent experiments performed in triplicate. * $P<0.05$; ** $P<0.01$; *** $P<0.001$.

Figure 6. **Expression of alternative mRNA variants *v2/v3*, encoding UGT1A_i2 proteins, is drastically reduced in human colon tumoral tissues. A)** Relative quantity (RQ) of alternative mRNA variants (*v2/v3)* expression in colon tumors compared to paired peritumoral normal tissues detected by quantitative PCR in 6 clinical samples. **B)** Quantification of mRNAs encoding UGT1A_i2 proteins by RNA sequencing (GSE80463) in normal and tumoral colon tissues. FPKM: Fragments Per Kilobase of transcript per Million mapped reads.

Figure 1

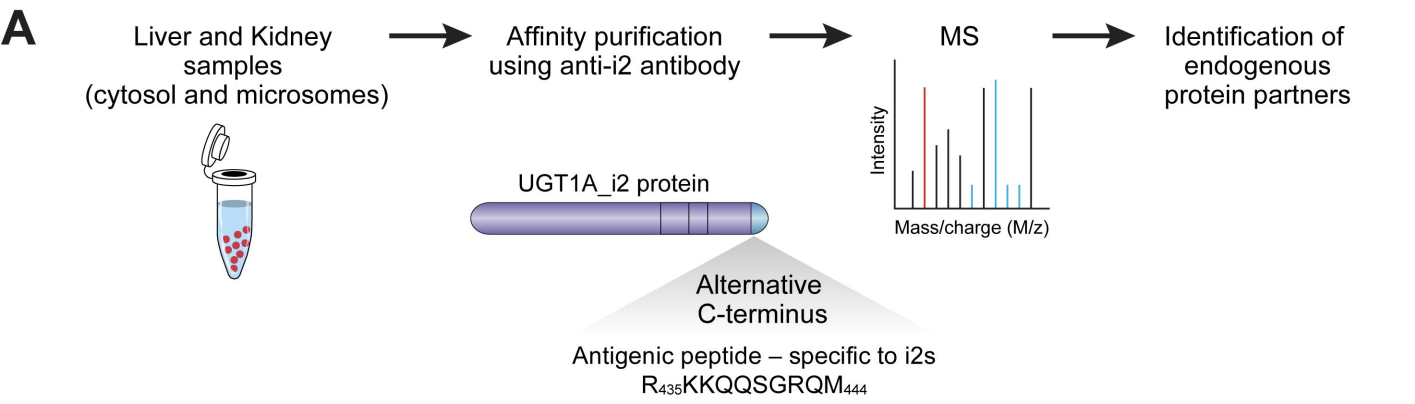
A
Liver and Kidney samples (cytosol and microsomes)
Affinity purification using anti-i2 antibody
MS
Identification of endogenous protein partners
Intensity
Mass/charge (M/z)
UGT1A_i2 protein
Alternative C-terminus
Antigenic peptide – specific to i2s
R435KKQQSGRQM444

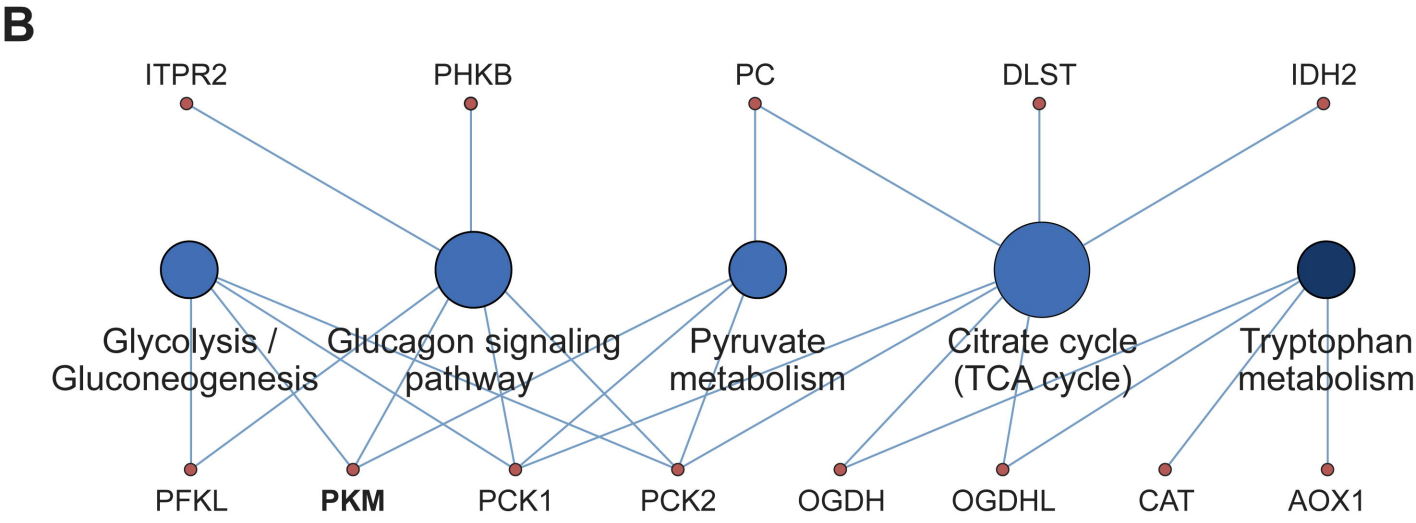
B
ITPR2
PHKB
PC
DLST
IDH2
Glycolysis / Gluconeogenesis
Glucagon signaling pathway
Pyruvate metabolism
Citrate cycle (TCA cycle)
Tryptophan metabolism
PFKL
PKM
PCK1
PCK2
OGDH
OGDHL
CAT
AOX1

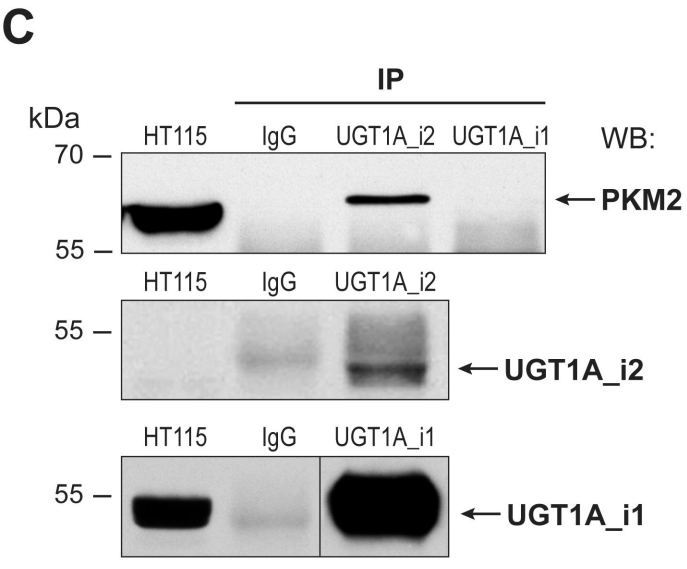
C
IP
kDa
HT115
IgG
UGT1A_i2
UGT1A_i1
WB:
70
55
PKM2
UGT1A_i2
UGT1A_i1

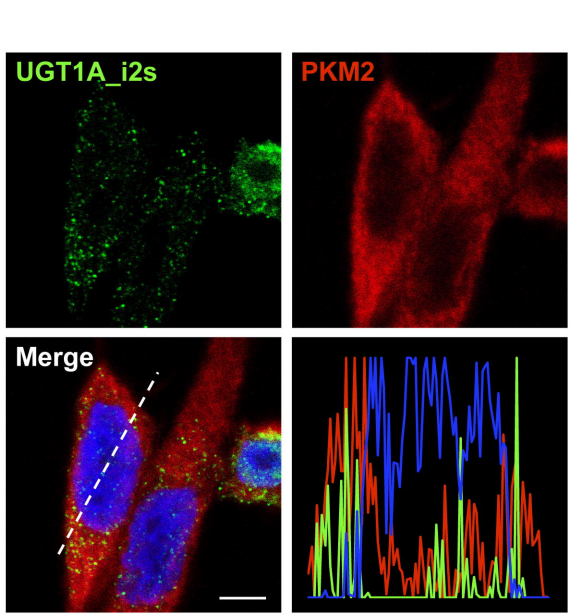
D
UGT1A_i2s
PKM2
Merge

Figure 2

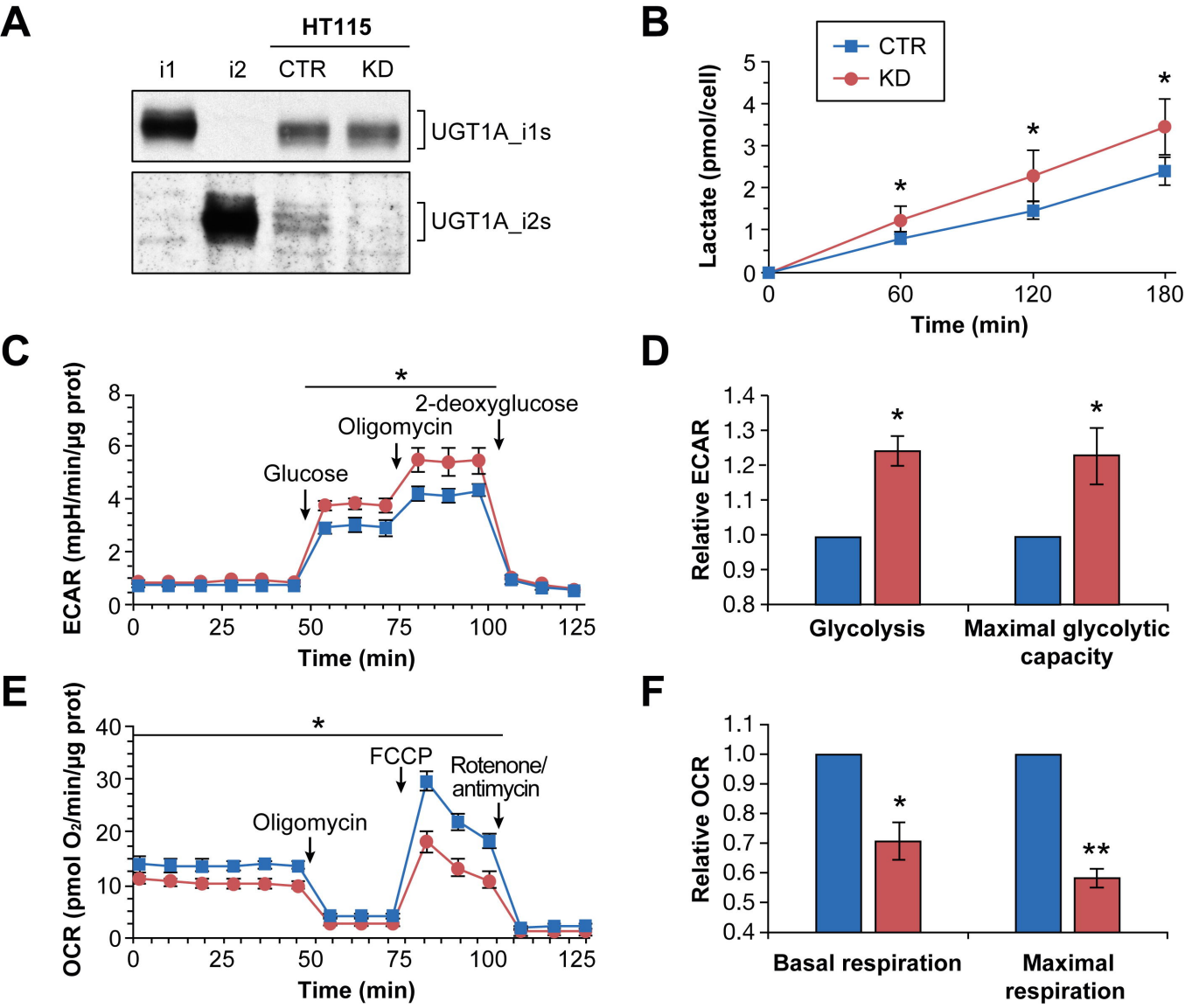
A
HT115
i1
i2
CTR
KD
UGT1A_i1s
UGT1A_i2s
B
CTR
KD
Lactate (pmol/cell)
Time (min)
C
ECAR (mpH/min/µg prot)
Glucose
Oligomycin
2-deoxyglucose
Time (min)
D
Relative ECAR
Glycolysis
Maximal glycolytic capacity
E
OCR (pmol O2/min/µg prot)
Oligomycin
FCCP
Rotenone/ antimycin
Time (min)
F
Relative OCR
Basal respiration
Maximal respiration

Figure 3

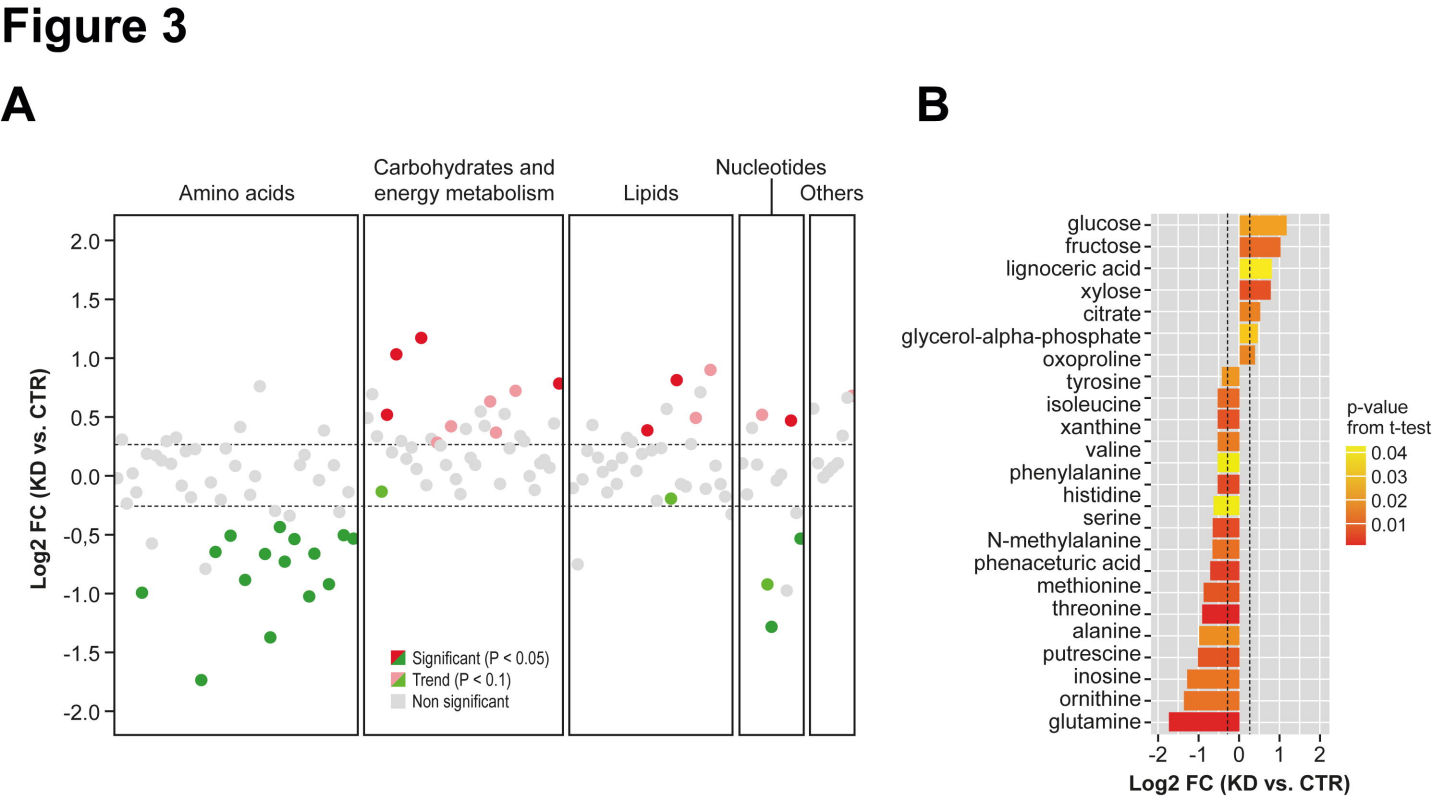
A
Amino acids
Carbohydrates and energy metabolism
Lipids
Nucleotides
Others
Log2 FC (KD vs. CTR)
2.0
1.5
1.0
0.5
0.0
-0.5
-1.0
-1.5
-2.0
Significant (P < 0.05)
Trend (P < 0.1)
Non significant
B
glucose
fructose
lignoceric acid
xylose
citrate
glycerol-alpha-phosphate
oxoproline
tyrosine
isoleucine
xanthine
valine
phenylalanine
histidine
serine
N-methylalanine
phenaceturic acid
methionine
threonine
alanine
putrescine
inosine
ornithine
glutamine
-2
-1
0
1
2
Log2 FC (KD vs. CTR)
p-value from t-test
0.04
0.03
0.02
0.01

Figure 4

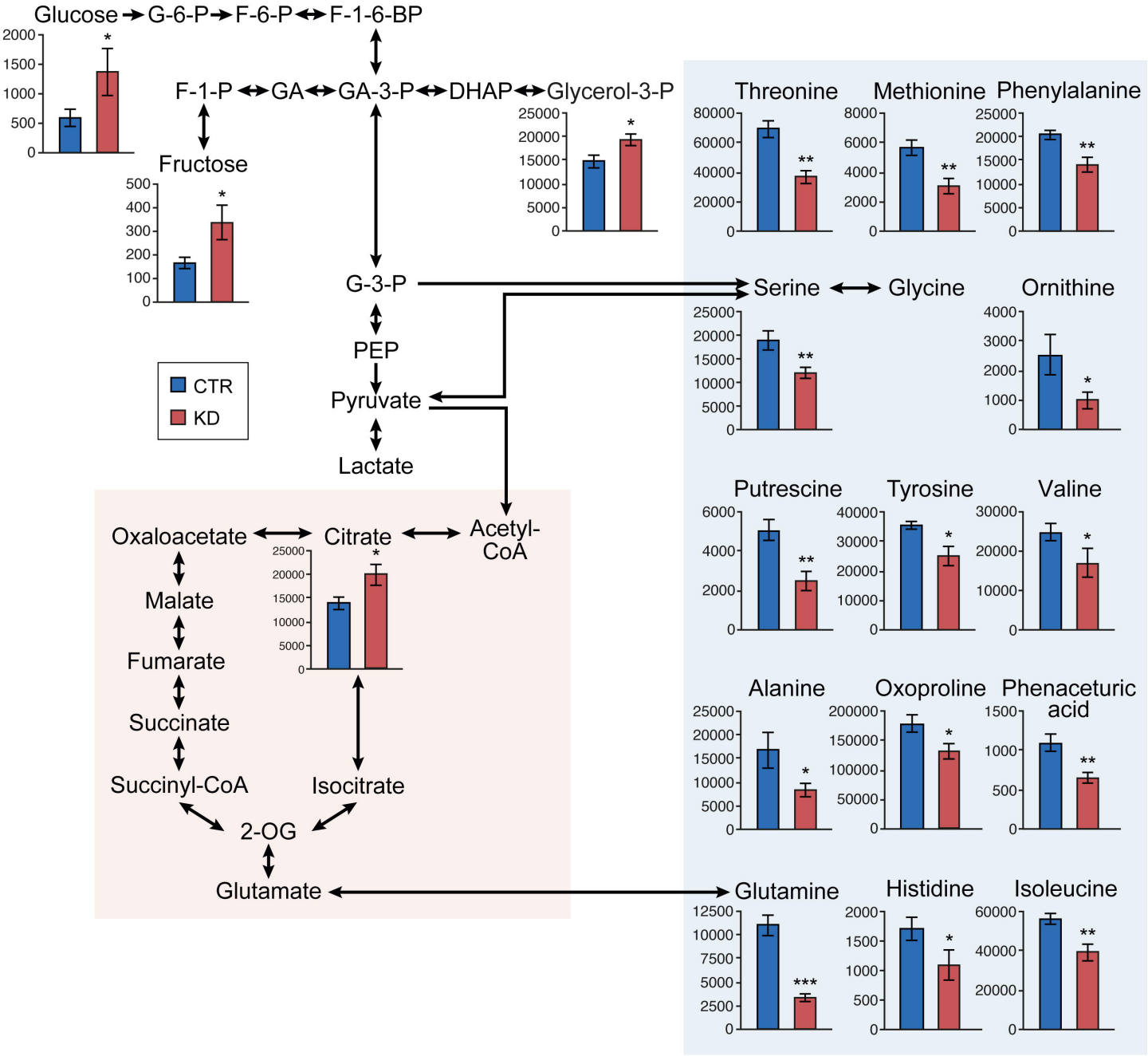
Glucose
G-6-P
F-6-P
F-1-6-BP
F-1-P
GA
GA-3-P
DHAP
Glycerol-3-P
Fructose
G-3-P
PEP
Pyruvate
Lactate
CTR
KD
Oxaloacetate
Citrate
Acetyl-CoA
Malate
Fumarate
Succinate
Succinyl-CoA
Isocitrate
2-OG
Glutamate
Threonine
Methionine
Phenylalanine
Serine
Glycine
Ornithine
Putrescine
Tyrosine
Valine
Alanine
Oxoproline
Phenaceturic acid
Glutamine
Histidine
Isoleucine

Figure 5

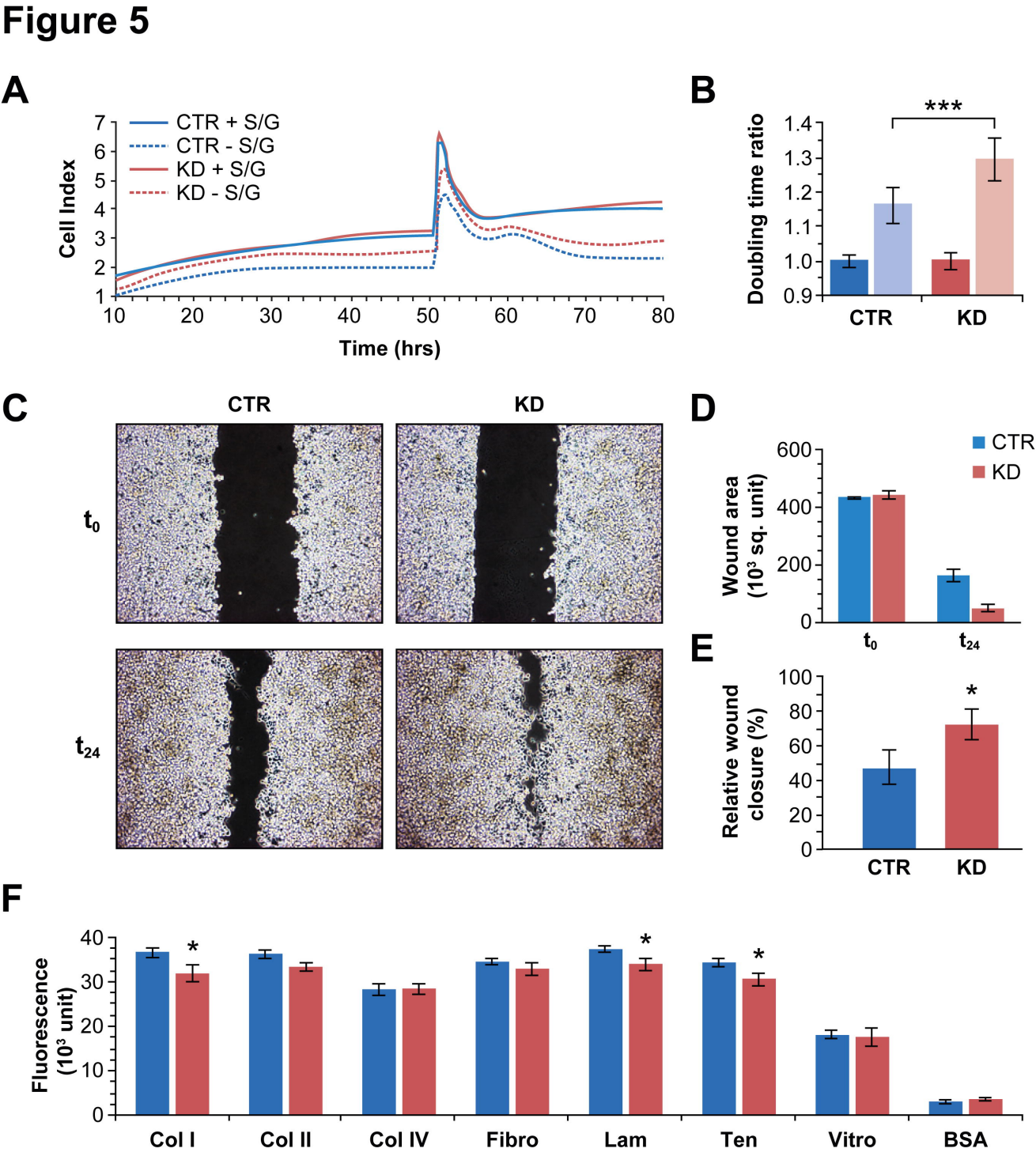
A
Cell Index
Time (hrs)
CTR + S/G
CTR - S/G
KD + S/G
KD - S/G
B
Doubling time ratio
***
CTR
KD
C
CTR
KD
t0
t24
D
Wound area (10³ sq. unit)
CTR
KD
t0
t24
E
Relative wound closure (%)
*
CTR
KD
F
Fluorescence (10³ unit)
Col I
Col II
Col IV
Fibro
Lam
Ten
Vitro
BSA

Figure 6

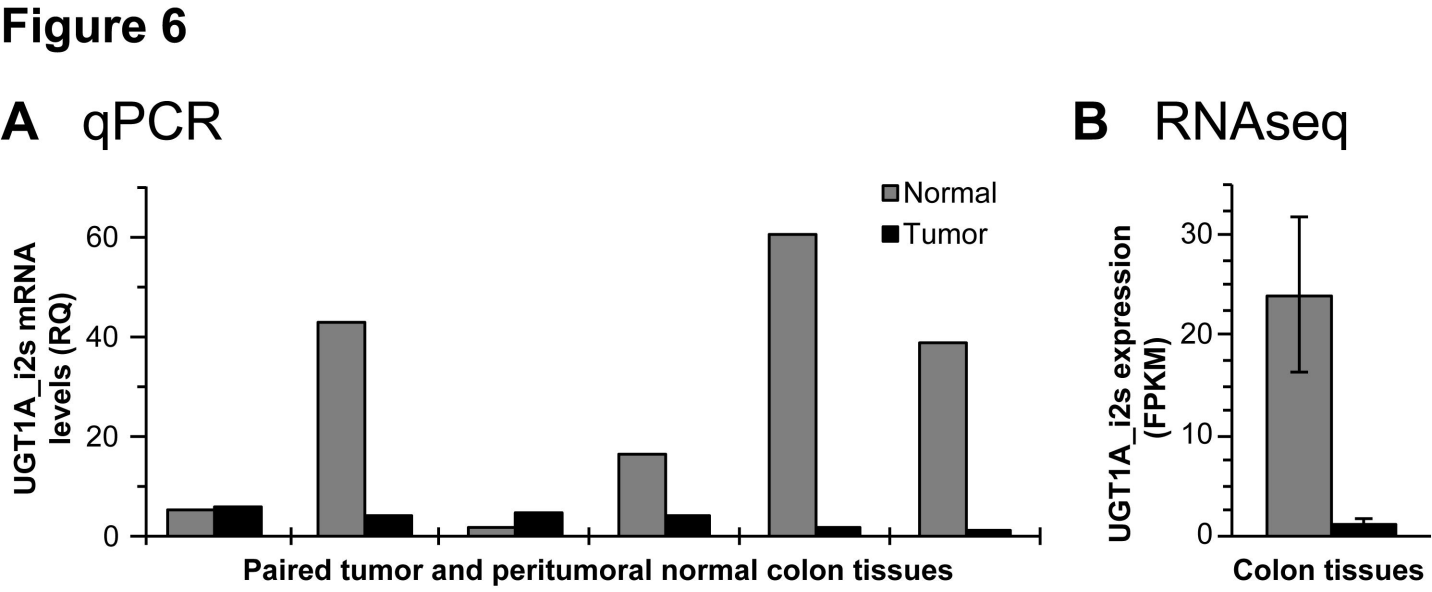
A qPCR
B RNAseq
Normal
Tumor
UGT1A_i2s mRNA levels (RQ)
0
20
40
60
Paired tumor and peritumoral normal colon tissues
UGT1A_i2s expression (FPKM)
0
10
20
30
Colon tissues